

# Strong form meshfree collocation method for frictional contact between a rigid pile and an elastic foundation

Ashkan Almasi<sup>1</sup> · Tae-Yeon Kim<sup>2</sup> · Jeong-Hoon Song<sup>1</sup> 

Received: 4 March 2022 / Accepted: 4 May 2022 / Published online: 30 May 2022  
© The Author(s), under exclusive licence to Springer-Verlag London Ltd., part of Springer Nature 2022

## Abstract

In this paper, a strong form meshfree collocation method is proposed for the frictional contact problem between a rigid pile and an elastic foundation. The method is based on the strong form of the governing equations and the meshfree collocation method. The contact problem is modeled as a boundary value problem with a unilateral constraint. The proposed method is applied to the problem of a rigid pile embedded in an elastic foundation. The results are compared with the finite element method (FEM) and the boundary element method (BEM). The proposed method is shown to be accurate and efficient.

**Keywords** S. IM. IP. IF. IS

## 1 Introduction

The problem of frictional contact between a rigid pile and an elastic foundation is a classic problem in engineering. It has been studied extensively in the literature. The problem is often modeled as a boundary value problem with a unilateral constraint. The proposed method is based on the strong form of the governing equations and the meshfree collocation method. The contact problem is modeled as a boundary value problem with a unilateral constraint. The proposed method is applied to the problem of a rigid pile embedded in an elastic foundation. The results are compared with the finite element method (FEM), the boundary element method (BEM), and the weighted residual method (WRM). The proposed method is shown to be accurate and efficient. The proposed method is compared with the FEM, BEM, and WRM. The proposed method is shown to be accurate and efficient. The proposed method is compared with the FEM, BEM, and WRM. The proposed method is shown to be accurate and efficient.

M . . . . .



...  $\epsilon_T > 0$  ...  $\mu$  ...  
 ... U ... E ...  
 ... :

A ... / ...  
 ... C ... F ...  
 ... C ...  
 ... :

1. T ...  
 ... :

...  $\mathbf{u}_T = (\mathbf{1} - \otimes) \mathbf{u} \quad \Gamma_c, N$  ...  
 ...  $t_N = \epsilon_N \langle g \rangle$  ...  
 E . (9).

2.

... I ...  
 ... T ...  
 ... A ...  
 ... T ...

B\_ ...  $\mathbf{a}(\bar{\mathbf{x}})$  ...  $L^2$ -

...  $\mathbf{M}$   $\mathbf{B}_m$  ...  $\hat{\mathbf{v}}$

...  $\mathbf{p}_m(\mathbf{x}_I; \bar{\mathbf{x}})$  ...  $\hat{\mathbf{v}}$  ... E . (20).  
 I E . (25), ...  $\mathbf{x} = \bar{\mathbf{x}}$  ...  $\mathbf{a}(\mathbf{x})$  ...  
 $\alpha u(\cdot)$  ...

...  $\alpha = (\alpha_1, \alpha_2) \in \mathbb{R}^2$  ... I  
 ... E . (28) ...

...  $\alpha_i \in \mathbb{R}^2$  ...  
 $\alpha_1 = (0, 0)$ ,

$$\mu \mathbf{n} \cdot \boldsymbol{\epsilon} + \lambda \mathbf{n} \cdot \mathbf{1}(\operatorname{div} \mathbf{u}) = \bar{\mathbf{t}} \quad \text{on } \Gamma_t \tag{36}$$

$$\mu(\mathbf{u}_{i,j} + \mathbf{u}_{j,i})\mathbf{n}_j + \lambda\delta_{ij}\mathbf{n}_j(\mathbf{u}_{k,k}) = \bar{\mathbf{t}}_i \quad \text{on } \Gamma_t \tag{37}$$

where  $\delta_{ij}$  is the Kronecker delta symbol. From Eqs. (28) and (37),

$$\sum_{j=1}^N \left\{ \lambda - 2\mu \phi_{IJ}^{1,0} n_1 - \mu \phi_{IJ}^{0,1} n_2 u_{1I} - \lambda \phi_{IJ}^{0,1} n_1 \mu \phi_{IJ}^{1,0} n_2 u_{2I} \right\} - t_1 x_I = 0, \tag{38}$$

$$\sum_{j=1}^N \left\{ \mu \phi_{IJ}^{0,1} n_1 - \lambda \phi_{IJ}^{1,0} n_2 u_{1I} - \lambda - 2\mu \phi_{IJ}^{0,1} n_2 \mu \phi_{IJ}^{1,0} n_1 u_{2I} \right\} - t_2 x_I = 0$$

for  $\mathbf{x}_j \in Y_c$ . From Eqs. (38) and (39), we can deduce that the PDM, (28) and (44) are satisfied for  $\mathbf{x}_j \in Y_c$ . From Eqs. (28) and (44),

$$\mathbf{x}_j \in Y_c \quad \mathbf{T} = \mathbf{0}$$

where  $\mathbf{R}$  is the reaction force vector. An arbitrary  $\mathbf{R}$  is chosen for  $j \in \mathbf{N}$ . From Eqs. (46) and (47),

$$\frac{\mathbf{R}}{u} = \mathbf{0}$$

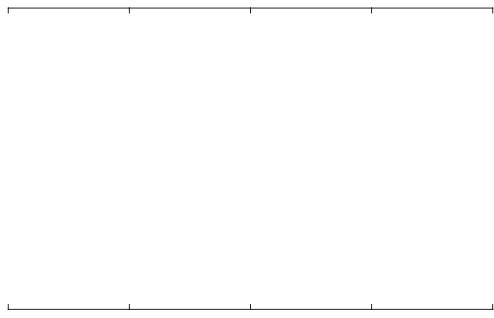
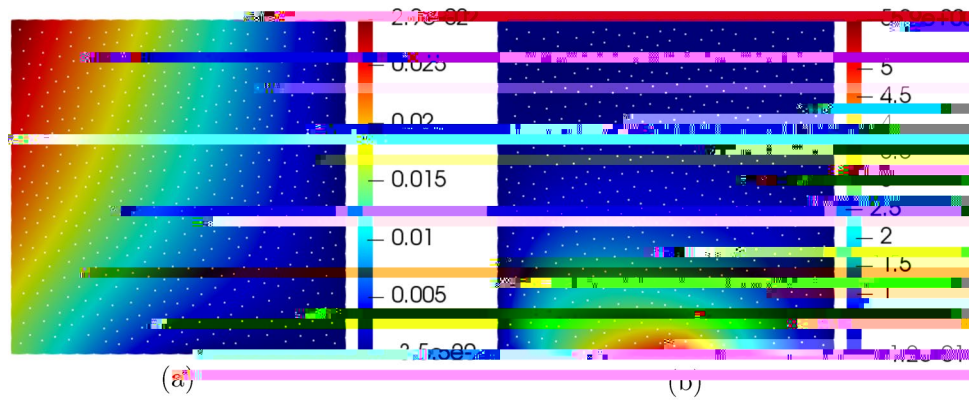
where  $j+1 \leq j \leq N$ . From Eqs. (46) and (47), we can deduce that  $\mathbf{R} = \mathbf{0}$  for  $j \in \mathbf{N}$ . From Eqs. (46) and (47),

$n$ .  $C$   
 $T = 10^{-12}$ .  $F$

$D$ ,  $N$ ,  $R$   
 $j + 1$ ,

1.  $C$

Fig. 4 D... a... b...  $\sigma_{xy}$ ,  $u_{xx}$



$\epsilon_N = \epsilon_T = 10^5 \text{ N}$  ...  
 F .2 ...  
 I F .3, ...  
 558 ...  
 T ...  $\Gamma_c$  ...  
 D ...  $u_{xx}$  ...  $\sigma_{xy}$  ...  
 F .4.A ...  
 T ... F .11 R ... F .44 .T ...  
 (COL) ... FEM ABAQUS ...  
 F .5.N ... H ... F .5 ...  
 Q ...

F .6 ... T ...





© The Author(s) 2023. **A**rticle number 13 (2023) 1–13

### 4.3 Hertzian contact problem

In [10], the authors proposed a numerical method for solving the Hertzian contact problem. The method is based on the finite element method (FEM) and the finite difference method (FDM). The authors used a 2D axisymmetric model of two elastic bodies in contact. The contact problem is solved by minimizing the total potential energy of the system. The authors used a Newton-Raphson iterative method to solve the nonlinear equations. The results show that the proposed method is accurate and efficient. The authors also compared their results with analytical solutions and other numerical methods. The proposed method is shown to be more accurate than the other methods. The authors also showed that the proposed method is more efficient than the other methods. The proposed method is suitable for solving the Hertzian contact problem.

H. [https://doi.org/10.1007/978-1-4939-9736-7\\_14](#) FEM [https://doi.org/10.1007/978-1-4939-9736-7\\_14](#)

#### 4.4 Frictional contact between a rigid pile and an elastic foundation



Fig. 19 C  $\sigma_{xx}$   $\sigma_{yy}$

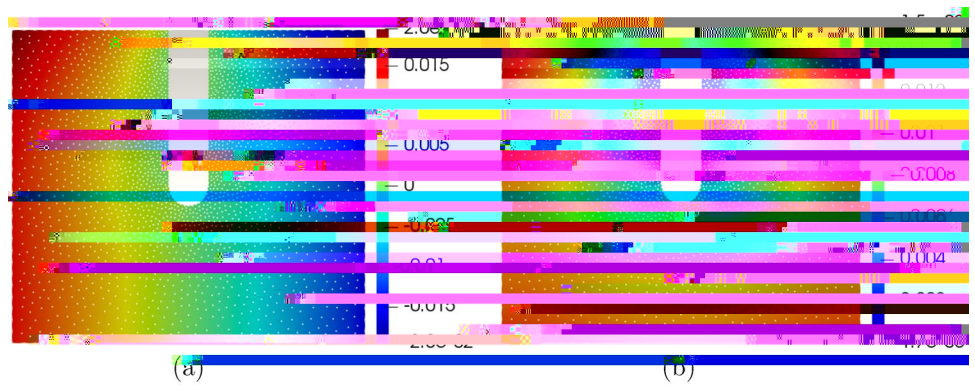


Fig. 20 C  $\sigma_{xx}$   $\sigma_{yy}$

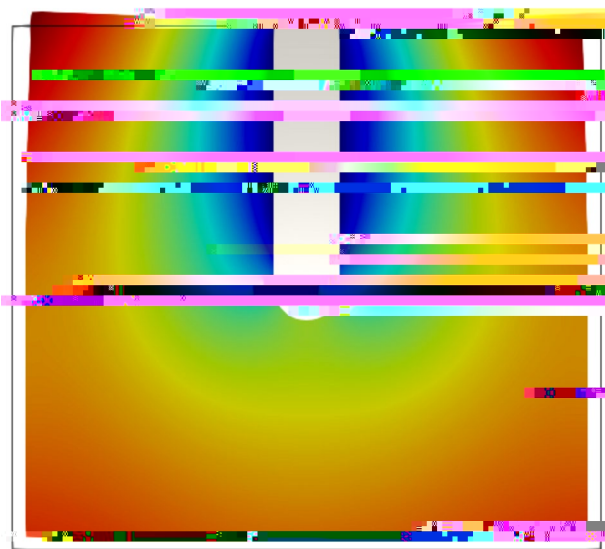
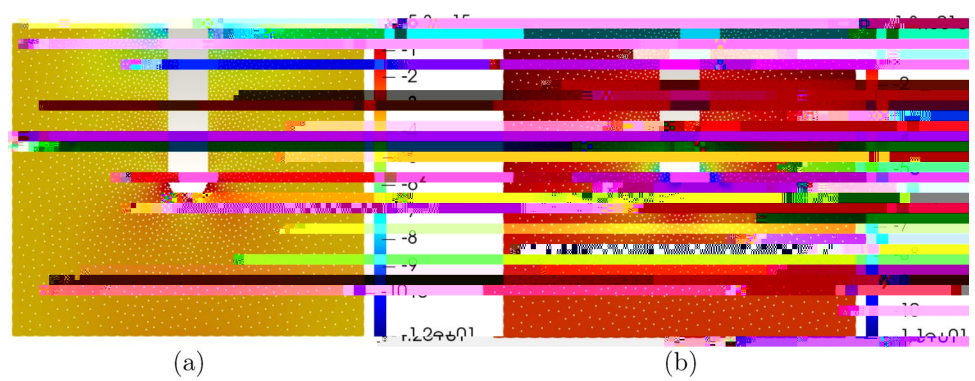


Fig. 21 C (15)

5 Conclusion

In this study, the finite element method (FEM) is used to analyze the stress distribution in a beam with a hole and a notch. The results show that the stress concentration is highest at the notch and lowest at the hole.

The finite element method (FEM) is a numerical technique used to solve problems in engineering and science. It is based on the principle of discretization, where a continuous domain is divided into a finite number of elements. The behavior of each element is approximated, and the overall behavior of the system is determined by combining the results of the individual elements. FEM is widely used in structural analysis, fluid dynamics, and heat transfer. In this study, FEM is used to analyze the stress distribution in a beam with a hole and a notch. The results show that the stress concentration is highest at the notch and lowest at the hole. This is due to the sharp change in geometry at the notch, which causes the stress lines to crowd together. The hole, on the other hand, causes the stress lines to spread out, resulting in a lower stress concentration. The finite element method (FEM) is a powerful tool for analyzing complex structures and systems. It allows engineers to simulate the behavior of a structure under various loading conditions and to identify areas of high stress concentration. In this study, FEM is used to analyze the stress distribution in a beam with a hole and a notch. The results show that the stress concentration is highest at the notch and lowest at the hole. This is due to the sharp change in geometry at the notch, which causes the stress lines to crowd together. The hole, on the other hand, causes the stress lines to spread out, resulting in a lower stress concentration. The finite element method (FEM) is a powerful tool for analyzing complex structures and systems. It allows engineers to simulate the behavior of a structure under various loading conditions and to identify areas of high stress concentration. In this study, FEM is used to analyze the stress distribution in a beam with a hole and a notch. The results show that the stress concentration is highest at the notch and lowest at the hole. This is due to the sharp change in geometry at the notch, which causes the stress lines to crowd together. The hole, on the other hand, causes the stress lines to spread out, resulting in a lower stress concentration.



T... ..  $K^c$  ... ..

$$(56) \quad T_{11J1}^N, K_{12J1}^N, K_{11J2}^N, K_{12J2}^N, K^{stick} \quad E \quad (57)$$

T... ..  $f_{stick}^c$  ... ..

T... ..  $K^c$  ... ..

T... ..  $K^{slip}$  E . (59)  $\mathbf{v}$  ... ..

T... ..  $f_{slip}^c$



26. L S, L WK (1999) R. . . . . I, JN . . . M. . . E 45(3):251–288

27. L S, L WK (1999) R. . . . . I, JN . . . M. . . E 45(3):289–317

28. K DW, K (2003) P. . . . . I, JN . . . M. . . E 56(10):1445–1464

29. L S-H, K K-H, -C (2016) P. . . . . I, JI . . . E 87:132–145

30. F . . . M. . . JG, S J-H (2017) B. . . . . J C . . . S 20:187–197

31. S J-H, F . . . K T- . . . -C, M. . . JG, R T (2018) P. . . . . I, J M. . . M. . . D. 14, 491–509. <https://doi.org/10.1007/10999-017-9386-1>

32. A . . . A, B . . . A, K T- . . . M. . . JG, S J-H (2019) S. . . . . J E M. . . 145(10):04019082

33. -C, S . . . P, R . . . T, S J-H (2019) N. . . . . E A B E. 98:310–327

34. B . . . A, K T- . . . L W, S J-H (2019) S. . . . . C . . . M. . . A M. . . E 351:404–421

35. C . . . J-S, W H-P (2000) N. . . . . C . . . M. . . A M. . . E 187(3–4):441–468

36. L G, B . . . T (2001) E. . . . . G . . . E C . . . 18(1/2):62–78

37. K J, G . . . B, G . . . JJ, K . . . E (2005) M. . . . . 2 . . . . . E A B E. 29(2):95–106

38. D. L . . . L, E . . . J, H . . . TJ, R. . . A (2015) I . . . . . N. . . . . C . . . M. . . A M. . . E 284:21–54

39. K . . . R, N 38.